Regular Article

PHYSICAL CHEMISTRY RESEARCH
Published by the
Iranian Chemical Society
www.physchemres.org
info@physchemres.org

***Phys. Chem. Res.**, Vol. 5, No. 4, 737-754, December 2017*
DOI: 10.22036/pcr.2017.87581.1381

A Density Functional Theory Investigation of d^8 Transition Metal(II) (Ni, Pd, Pt) Chloride Complexes of Some Vic-dioximes Derivatives

L. Ngouo Nogheu[a], J. Numbonui Ghogomu[a,*], N. Kennet Nkungli[a], D. Bikélé Mama[b] and E. Younang[c]

[a]*Department of Chemistry, Faculty of Science, University of Dschang, Dschang, Cameroon*
[b]*Department of Chemistry, Faculty of Science, University of Douala, Douala, Cameroon*
[c]*Department of Inorganic Chemistry, Faculty of Science, University of Yaounde I, Yaounde, Cameroon*

(Received 28 May 2017, Accepted 6 August 2017)

Herein, a theoretical study on the stability of some vic-dioxime complexes of Ni(II), Pd(II) and Pt(II) in gas and aqueous phases is reported. The DFT/M06/SDD and DFT/M06/6-31G+(d,p) levels of theory were adopted for the metal ions and for other elements, respectively. Structural analyses of investigated complexes have revealed square planar geometries stabilized by two O-H···Cl hydrogen bonds. Analysis of hydrogen bond energies calculated *via* quantum theory of atoms in molecules (QTAIM) and computed chemical hardness values have revealed that the stability of the complexes is determined by the hydrogen bond strength. Natural population analysis has revealed ligand-metal charge transfer in the complexes investigated. A good linear agreement with correlation coefficient 0.992 has been found between calculated and experimental IR vibrational frequencies, indicating the validity of the theoretical method employed herein. Negative binding energies obtained are indicative of the stability of the complexes, affirming the use of vic-dioximes ligands as potential d^8 transition metal eliminating agents in solution.

Keywords: DFT, Vic-dioxime complexes, QTAIM

INTRODUCTION

The potentials of vicinal dioximes ligands in the formation of coordination compounds continue to attract a great deal of research interest as a result of their applications in dioxygen carriers [1], catalysis [2-3], intramolecular hydrogen bonding and metal-metal interactions [4-5]. In addition, stable complexes prepared with vic-dioxime ligands have been used extensively for different purposes and in areas such as pigments and electrooptical sensors, analytical and medicinal chemistry, and biochemistry. [6] Dioximates of metals from nickel triad are used as electroluminescent substances in the production of light emitting diodes (LED) because of their crystallization properties. The stable planar structures of dioximes complexes result from H-bond formation [7] and, thereby, exhibit important electronic properties. Moreover, their high stability has been extensively exploited for various purposes including model compounds for vitamin B12, inhibitors of enzymes and intermediates in the biosynthesis of nitrogen oxides and model compounds for trace metal analysis [8-11]. To the best of our knowledge from the literature, much experimental work has been carried out on vic-dioximes but less theoretical effort has been devoted toward their d^8 metal eliminating ability [12-13].

Environmental pollution by d^8 transition metal ions is a public health problem as they are responsible for many water-borne diseases. Good enough, dioximes and their metal complexes meet applications in the area of coordination chemistry. Nowadays, dioximes and their derivatives are used in the conception of some sensors used for the trace determination of Ni, Pd and Co in the water bodies such as lakes, oceans and different biological systems [14-15].

*Corresponding author. E-mail: ghogsjuju@hotmail.com

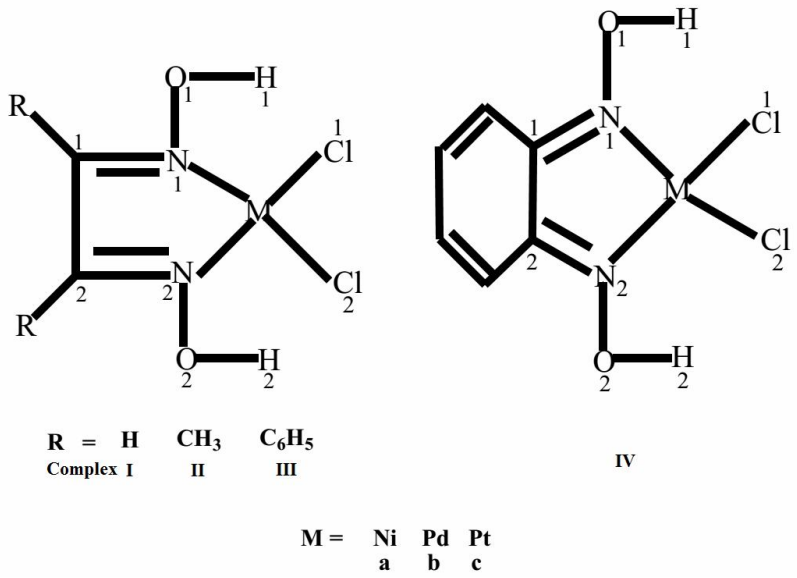

Fig. 1. Different complexes envisaged. Legend: I: dichloroglyoxime metal(II); II: dichlorodimethylglyoxime metal(II); III: dichlorodiphenylglyoxime metal(II); IV: dichlorocyclohexa-3,4-diene-1,2-dionedioxime metal(II). a: Nickel(II), b: Palladium(II) and c: Platinium(II).

In a previous theoretical study on the thermodynamic properties of some 3d (Fe, Co, Ni and Cu) metal(II) chloride complexes of glyoxime and its derivatives using DFT [16], it was shown that Ni(II) ions exhibit the greatest affinity toward the ligands (vic-dioximes and chloride ions). On this basis, the present work has been stablished to verify the stability of some vic-dioxime complexes of d^8 metal ions of the same group as Ni(II). Furthermore, vic-dioximes are well-known selective gravimetric reagents for the determination of nickel and palladium [17]. To gain more insight into the molecular properties of the oxime-metal complexes as well as to improve upon dioxime-based analytical procedures and reagents, this work has been set up to theoretically investigate the Ni(II), Pd(II) and Pt(II) ion chelating ability of a series of vic-dioxime ligands.

To accomplish this goal, density functional theory (DFT) studies have been undertaken on some vic-dioximes ligands and their d^8; Ni(II), Pd(II) and Pt(II) chloride complexes in the gas and aqueous phases. The atomic labeling scheme adopted herein for the investigated complexes is shown in Fig. 1. Specifically, geometrical parameters (bond lengths, bond angles and dihedral angles) around the central metal ions, along with hydrogen bond (O-H···Cl) parameters have been studied. Furthermore, atomic charges have been computed via natural population analysis (NPA) in order to investigate the metal-ligand charge transfer pattern in the complexes studied. Moreover, reactivity of the envisaged complexes has been described in terms of the chemical reactivity descriptors obtained from vertical electron affinity and ionization energy. To determine the ligand affinities for the metal ions studied, metal-ligand binding energies, Gibbs free energies and enthalpy changes of complexation have been investigated. QTAIM analyses [18-19] have been carried out on the complexes in order to shed more light on the nature of the O-H···Cl H-bonds. The DFT method has been chosen for this study due to its success story in modeling metal complexes, coupled with its remarkable accuracy and computational time ratio [20].

COMPUTATIONAL DETAILS

All DFT calculations were performed with the Gaussian 09 package [21]. The input structures were prepared using the GaussView 5.0.8 program [22]. The Minnesota functional M06 [23] was used to approximate the exchange-

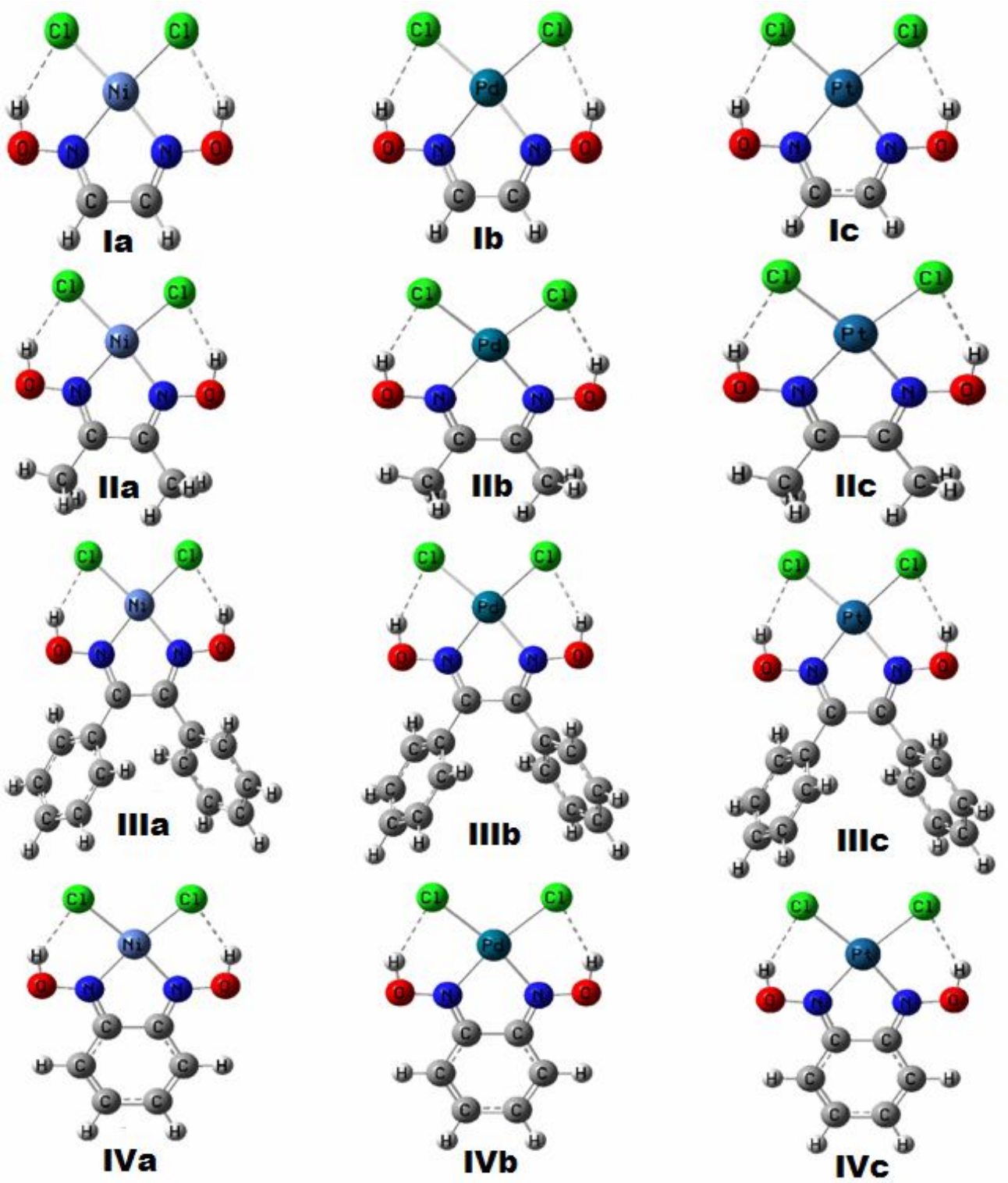

Fig. 2. Gas-phase optimized geometries of the investigated complexes obtained at the M06/6-31+G(d,p) level of theory, and SDD basis set for metal (II). Structures were visualized using GaussView 5.0.8.

correlation energy. This functional was chosen because it describes long-range dispersion interactions properly, and is thus one of the best functionals for the study of organometallic and inorganometallic thermochemistry, as well as systems containing hydrogen bonds [23]. The SDD (Stuttgart-Dresden) [24] ECP/basis set was used for the central metal ions, whereas the Pople-style basis set 6-31+G(d,p) was used for all other elements. Geometry optimizations were performed without symmetry constraint of any kind. To confirm the optimized geometries as global minima on their potential energy surfaces, harmonic vibration frequencies were calculated at the same level of theory as that used for geometry optimization. No imaginary frequency was found for all complexes investigated, ascertaining that a true minimum on the potential energy surface was obtained in each case. The restricted closed-shell Kohn-Sham model was adopted for the complexes, which were treated as low spin species. Solvent effects were accounted for *via* the polarized continuum salvation model (PCM) coupled with the integral equation formalism (IEF) approach [25]. The Bader's quantum theory of atoms in molecules (QTAIM) [13] was performed with multiwfn [26].

RESULTS AND DISCUSSION

Structural Analysis

The optimized geometries in gas phase adopted for the investigated complexes are shown in Fig. 2. Some selected gas and solvent phase bond lengths, bond angles and dihedral angles of the d^8 transition metal(II) chloride complexes of vic-dioximes, optimized at M06/6-31+G(d,p)/(SDD for metal ions) level of theory, are listed in Table 1 for comparison. It is evidenced from this table that the lengths of M-N bonds increase in the order: Ni-N < Pt-N < Pd-N for all cases studied. Furthermore, the lengths of the M-Cl bonds (2.147-2.331 Å) are found to increase in the same order as the atomic number (Z) of the central metal(II) ions ($Z_{Ni^{2+}} < Z_{Pd^{2+}} < Z_{Pt^{2+}}$). It is clear from these results that the metal-ligand bonds are shorter and probably stronger in Ni^{2+} complexes than those in the rest of the complexes studied.

Inspection of Table 1 shows that the lengths of the O-H···Cl H-bonds in the complexes studied (in each medium) are affected by the nature of the central metal ion. Indeed, the lengths of these H-bonds are shortest in Ni^{2+} complexes and longest in Pt^{2+} complexes. A possible explanation for this observation is linked to the values of the N-M-Cl angles which are dependent on the nature of the central metal. From Fig. 1, it can be seen that a reduction in the N-M-Cl angle will lead to a reduction in the corresponding O-H···Cl H-bond length. The values of the N-M-Cl angles are found to be smallest in Ni^{2+} complexes (91.35°-92.03° in gas phase and 92.06°-92.74° in water) and largest in Pt^{2+} complexes (92.11°-92.68° in gas phase and 92.87°-93.57° in water), indicating that the O-H···Cl H-bonds are shortest/strongest in the former complexes, and are longest/weakest in the latter. The planarity of these complexes, which can be judged from the values of the dihedral angles M-N_1-C_1-C_2, can affect the strength of the O-H···Cl H-bonds and consequently the stability of each complex. The more planar the complexes are, the shorter and stronger these H-bonds become. For each complex, the value of this angle is close to 0°, signifying that the complexes adopt nearly planar geometries around central metal ions.

Thermodynamic Parameters of the Investigated Complexes

In an effort to predict the d^8 metal-binding potentials of the vic-dioximes ligands investigated, their d^8 metal-coordinating abilities were determined via the following thermodynamic parameters of complexation: binding energy (ΔE), enthalpy change (ΔH^o) and Gibbs free energy change (ΔG^o). These parameters were calculated according to Eqs. (1)-(3). The numerical values of E, G^o and H^o used in these equations were computed through thermochemical analysis at 298.15 K and 1 atm, in both gas and water phases. Thermochemical analyses were performed using the default settings of Gaussian 09, which employ the harmonic oscillator approximation in the computation of IR frequencies. Binding energies were computed using thermal energies, which incorporate zero-point vibrational corrections.

$$\Delta E = E_{complex} - (E_{ligand} + E_{metal} + 2E_{Cl}) \quad (1)$$

Table 1. Some Selected Optimized Bond Lengths (Å), Bond Angles (°) and Dihedral Angles (°) of Metal d^8 Vic-dioximes Complexes at the M06/6-31+G(d,p) Level of Theory, and SDD Basis Set for Metal(II)

Molecules	d(M-N)	d(M-Cl)	d(O-H)	d(H···Cl)	ɵ(N_1-M-Cl_2)	Φ (M-N_1-C_1-C_2)
			Gas			
Ia	1.910	2.147	0.995	2.126	91.35	0.00000
Ib	2.040	2.296	0.991	2.283	91.62	0.00000
Ic	2.017	2.323	0.990	2.295	92.11	0.00000
IIa	1.907	2.153	0.994	2.114	91.94	0.00347
IIb	2.028	2.302	0.991	2.247	92.18	-0.00702
IIc	2.009	2.330	0.990	2.261	92.59	-0.00175
IIIa	1.900	2.155	0.995	2.087	92.03	-3.93545
IIIb	2.022	2.320	0.994	2.229	92.34	-3.16453
IIIc	2.009	2.331	0.990	2.247	92.68	-2.44718
IVa	1.900	2.150	0.994	2.120	91.40	0.00249
IVb	2.028	2.298	0.991	2.266	91.60	-0.00066
IVc	2.006	2.325	0.989	2.288	92.25	0.00026
			Water			
Ia	1.909	2.171	0.987	2.183	92.11	0.00000
Ib	2.038	2.322	0.984	2.357	92.41	0.00000
Ic	2.019	2.356	0.984	2.359	92.88	0.00000
IIa	1.907	2.153	0.995	2.115	92.17	0.00694
IIb	2.024	2.330	0.984	2.317	93.06	-0.02329
IIc	2.017	2.362	0.983	2.347	93.57	-0.00038
IIIa	1.899	2.178	0.988	2.143	92.74	-5.17851
IIIb	2.027	2.328	0.985	2.304	92.98	-1.85172
IIIc	2.010	2.362	0.984	2.315	93.46	-1.58864
IVa	1.900	2.174	0.987	2.172	92.06	0.00248
IVb	2.026	2.325	0.984	2.335	92.40	0.00000
IVc	2.008	2.359	0.984	2.343	92.87	-0.00619

$$\Delta G^{\circ} = G^{\circ}_{complex} - (G^{\circ}_{ligand} + G^{\circ}_{metal} + 2G^{\circ}_{Cl}) \quad (2)$$

$$\Delta H^{\circ} = H^{\circ}_{complex} - (H^{\circ}_{ligand} + H^{\circ}_{metal} + 2H^{\circ}_{Cl}) \quad (3)$$

From the values of ΔE, ΔH^o and ΔG^o calculated at M06/6-31+G(d,p)/(SDD for metal ions) level of theory, listed in Table 2, it is clear that all binding energies are negative in the gas phase and in water, implying that the complexation reactions are favorable in both media. For all vic-dioximes ligands and metal ions investigated, the calculated ΔE values for the formation of the complexes increase in the order: $\Delta E_{IV} < \Delta E_{II} < \Delta E_{I} < \Delta E_{III}$. This ranking is corroborated by the calculated values of ΔH^o and ΔG^o. According to these results, the formation of complex IV from cyclohexa-3,5-diene-1,2-dione dioxime and Pt^{2+}, Pd^{2+} or Ni^{2+} is most favorable, while the formation of complex III from diphenylglyoxime and each of these metal ions is least favorable. From Table 2, it is evidenced that for each vic-dioxime ligand studied, the metal ion selectivity decreases in the order: $Pt^{2+} > Pd^{2+} \geq Ni^{2+}$ in gas phase and $Pd^{2+} > Ni^{2+} > Pt^{2+}$ in solution, since the values of ΔE, ΔH^o and ΔG^o follow this ranking in the respective media.

Based on the values of ΔG^o, the complexation reactions are much more favorable in gas phase than in water. This is probably due to the interactions with solvent molecules. From the highly negative values of ΔE, ΔH^o and ΔG^o obtained in this work, it can be concluded that vic-dioximes are promising d^8 metal-binding ligands. Among the ligands investigated, cyclohexa-3,5-diene-1,2-dione dioxime exhibits a remarkable d^8 metal-binding ability than all the rest.

Natural Population Analysis (NPA)

In order to determine the nature of metal-ligand charge transfer in the complexes under investigation, atomic charges were computed using the NPA atomic charge scheme. This scheme was chosen because it is not significantly affected by basis set size. The calculated NPA charges on the central metal ions in the complexes investigated are presented in Table 3. By careful inspection of this table, it can be seen that upon coordination with the ligands the positive charges on the central metal ions (0.302-0.330 in the gas phase and 0.362-0.399 in water) are decreased significantly from their formal +2 charge. This is indicative of significant electron transfer from the ligands to the metal ions during complexation. It is also clear from Table 3 that the charges on the various metal ions in water as solvent are larger than those in the gas phase, indicating that ligand-to-metal charge transfer is more effective in gas phase than in solvent phase. This observation is corroborated by the strong metal-ligand interactions in the gas phase, which are characterized by lower binding energies compared to those calculated in water, as discussed in section 3.2. This significant ligand-to-metal charge transfer is likely to strengthen the binding of the metal ions studied by the vic-dioximes ligands.

Chemical Reactivity Descriptors

The DFT approach provides a sound theoretical basis for the determination of the ionization potential (IP) and electron affinity (EA).

$$IP = E_{(N-1)} - E_{(N)} \quad (4)$$

$$EA = E_{(N)} - E_{(N+1)} \quad (5)$$

where, $E_{(N)}$, $E_{(N-1)}$ and $E_{(N+1)}$ are the energies of the parent molecule and its cationic and anionic radicals, respectively. In this work, vertical ionization potential (IP_V) and vertical electron affinity (EA_V) have been computed. In this case, $E_{(N)}$, $E_{(N-1)}$ and $E_{(N+1)}$ are single point energies of the neutral molecule, and its cationic and anionic species, respectively, calculated at the geometry of the neutral molecule. It is important to note that IP_V is the energy needed to remove an electron from a molecule, whereas EA_V measures the ability of a molecule to accept electrons [27].

In the realm of conceptual DFT, the values of IP_V and EA_V are used to describe molecular reactivity in terms of global reactivity descriptors such as the global hardness (η). The global hardness (calculated as shown in equation (6)) is a measure of the resistance to charge transfer [27].

$$\eta = 1/2\ (IP_V - EA_V) \quad (6)$$

The values of η calculated in both gas and solvent phases

Table 2. Main Energy Parameters of Metal d^8 Vic-dioximes Complexes in kcal mol^{-1} at the M06/6-31+G(d,p) Level of Theory, and SDD Basis Set for Metal(II)

		Gas			Water		
Vic-dioxime ligands	Complexes	ΔH^o	ΔG^o	ΔE	ΔH^o	ΔG^o	ΔE
Glyoxime	Ia	-719	-692	-717	-162	-135	-160
	Ib	-720	-694	-718	-167	-141	-165
	Ic	-738	-711	-736	-146	-120	-144
Dimethylglyoxime	IIa	-724	-697	-722	-153	-126	-151
	IIb	-724	-698	-722	-171	-145	-169
	IIc	-741	-714	-739	-149	-123	-148
Diphenylglyoxime	IIIa	-716	-688	-714	-158	-129	-156
	IIIb	-716	-689	-714	-161	-135	-159
	IIIc	-734	-706	-732	-140	-114	-138
Cyclohexa-3,5-diene-1,2-dione dioxime	IVa	-724	-696	-723	-166	-139	-164
	IVb	-726	-698	-724	-171	-144	-169
	IVc	-745	-716	-743	-151	-124	-149

Table 3. Variation of Natural Population Atomic Charges at the M06/6-31+G(d,p) Level of Theory, and SDD Basis Set for Metal (II)

	Medium	Ia	Ib	Ic	IIa	IIb	IIc	IIIa	IIIb	IIIc	IVa	IVb	IVc
Charge on the metal ions	Gas	0.317	0.315	0.310	0.323	0.310	0.302	0.327	0.316	0.309	0.327	0.325	0.330
	Water	0.390	0.379	0.382	0.366	0.368	0.362	0.394	0.379	0.378	0.394	0.384	0.399

are listed in Table 4. A careful examination of this table revealed that the IP values of the complexes Ia-Ic decrease in the order: Pd(II) complexes > Ni(II) complexes > Pt(II) complexes in both gas and solvent phases. The same trend was observed for the complexes IIa-IIc, IIIa-IIIc and IVa-IVc. Therefore, among the complexes studied, the Pd(II) complexes are not easily oxidized owing to their high ionization potentials. It is also clear from Table 4 that the EA_V values of the Pt(II) and Pd(II) complexes in the gas and aqueous phases are higher than those of the Ni(II) complexes in nearly all cases studied. This shows that the Ni(II) complexes can be easily reduced in gas and aqueous

Table 4. Values of the Global Reactivity Descriptors of the Systems in eV Calculated at the M06/6-31+G(d,p) Level of Theory, and SDD Basis Set for Metal(II)

Molecules	Gas			Water		
	EA_v	IP_v	η	EA_v	IP_v	η
Ia	-2.14	9.27	5.71	-4.08	7.24	5.66
Ib	-1.68	9.32	5.50	-3.61	7.36	5.49
Ic	-2.01	9.10	5.56	-3.55	7.03	5.29
IIa	-1.86	8.85	5.35	-4.36	6.47	5.41
IIb	-1.41	8.94	5.17	-3.45	7.19	5.32
IIc	-1.59	8.69	5.14	-3.15	6.86	5.00
IIIa	-1.93	8.48	5.21	-4.00	7.03	5.52
IIIb	-1.96	8.57	5.26	-3.54	7.11	5.32
IIIc	-1.98	8.36	5.17	-3.47	7.02	5.25
IVa	-2.66	8.58	5.62	-4.16	6.64	5.40
IVb	-2.71	8.62	5.66	-4.16	6.66	5.41
IVc	-2.69	8.45	5.57	-4.15	6.51	5.33

media than the Pt(II) and Pd(II) counterparts whose EA_V values are relatively higher. In most cases studied, the Ni(II) complexes are found to have the highest η values. In fact, the η values of the complexes decrease in the order: Ni(II) complexes > Pd(II) complexes > Pt(II) complexes. Consequently, the Ni(II) complexes are the most kinetically stable and the least chemically reactive.

QTAIM Investigation of H-bonds

In order to characterize the metal-ligand and H-bond interactions in the currently investigated complexes, the topological analyses of their electron densities have been carried out in the framework of the quantum theory of atoms in molecules (QTAIM) proposed by Bader and coworkers [28-31]. In this regard, analyses of electron density $\rho(\boldsymbol{r})$ and its Laplacian $\nabla^2\rho(\boldsymbol{r})$ were performed at bond critical points (BCP). It is worthy of note that at the BCP, $\nabla\rho(\boldsymbol{r}) = 0$. The sign of $\nabla^2\rho(\boldsymbol{r})$ at a BCP reveals whether charge is concentrated in the interatomic space as in covalent bonds ($\nabla^2\rho(\boldsymbol{r}) < 0$), or depleted as in closed shell (electrostatic)

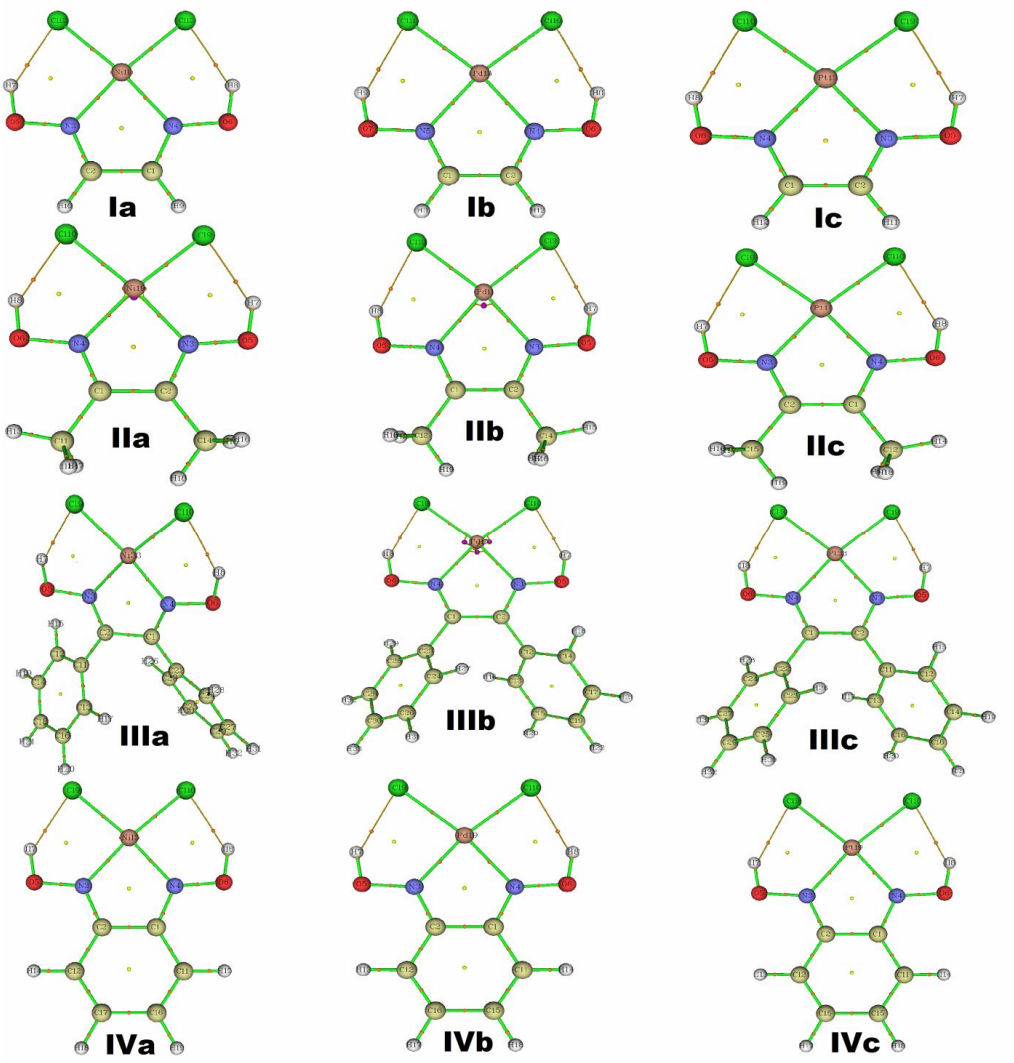

Fig. 3. Molecular graphs of the complexes studied in the gas phase: the tiny red and yellow spheres represent bond and ring critical points, respectively, whereas the green lines are bond paths.

interactions ($\nabla^2\rho(\boldsymbol{r}) > 0$). Generally, $\rho(r)$ at the BCP is greater than 0.2 a.u. in shared (covalent) bonding interactions and less than 0.1 a.u. in closed-shell interactions (ionic, van der Waals, H-bonding) [32]. The sign of the energy density, $H(\boldsymbol{r})$, determines whether the accumulation of charge at a given point $\boldsymbol{r}$ is stabilizing ($H(\boldsymbol{r}) < 0$) or destabilizing ($H(r) > 0$). In this work, bonding interactions were also characterized using the ratio $-G(r)/V(r)$. Generally, when $-G(r)/V(r) > 1$ the bonding interaction concerned is noncovalent, whereas when $0.5 < -G(r)/V(r) < 1$ the interaction is partially covalent. The topological parameters for the d^8 metal - vic-dioximes complexes calculated in the gas phase and in water are listed in Tables 5 and 6, respectively. Koch and Popelier [33] proposed certain criteria for H-bond formation, among which, a BCP must be present between the hydrogen atom and the acceptor atom.

In each molecule studied, the two intramolecular H-bonds (O-H···Cl) have been confirmed by the existence of a BCP between the donor O-H groups and the acceptor chloride ions**,** as shown in Fig. 3. According to the values in Tables 5 and 6, electron density at the BCPs of the H-bonds

Table 5. Topological Analysis of H-bonds (O-H···Cl) and M-N Bonds of the Complexes Studied in the Gas Phase

Complexes	Interactions	$\rho(r)$	$\nabla^2\rho(r)$	$H(r)$	$-G(r)/V(r)$	E (kJ mol^{-1})
			O-H···Cl/M-N			
Ia	OH···Cl	0.0265	0.0687	-0.00096	0.95	-24.9
	M-N	0.101	0.542	-0.0135	0.92	-212.7
Ib	OH···Cl	0.0181	0.0518	0.00049	1.04	-15.8
	M-N	0.104	0.481	-0.0202	0.87	-211.5
Ic	OH···Cl	0.0179	0.0520	0.000531	1.05	-15.6
	M-N	0.122	0.502	-0.0360	0.82	-258.6
IIa	OH···Cl	0.0313	0.728	-0.00207	0.91	-29.4
	M-N	0.104	0.564	-0.0154	0.91	-225.8
IIb	OH···Cl	0.0188	0.0533	0.000367	1.03	-16.5
	M-N	0.107	0.491	-0.0225	0.86	-220.5
IIc	OH···Cl	0.0184	0.0529	0.000447	1.04	-16.2
	M-N	0.124	0.507	-0.0381	0.81	-266.5
IIIa	OH···Cl	0.0288	0.0726	-0.00143	0.94	-27.4
	M-N	0.104	0.550	-0.0158	0.91	-221.9
IIIb	OH···Cl	0.0202	0.0554	0.000108	1.01	-17.9
	M-N	0.107	0.490	-0.0221	0.87	-219.2
IIIc	OH···Cl	0.0197	0.0549	0.000217	1.02	-17.5
	M-N	0.124	0.510	-0.0383	0.81	-267.8
IVa	OH···Cl	0.0271	0.0699	-0.00108	0.94	-25.7
	M-N	0.104	0.549	-0.0155	0.91	-220.5
IVb	OH···Cl	0.0189	0.0534	0.000345	1.02	-16.7
	M-N	0.107	0.491	-0.0222	0.87	-219.2
IVc	OH···Cl	0.0186	0.0532	0.000422	1.03	-16.4
	M-N	0.125	0.510	-0.390	0.81	-269.1

in all the complexes investigated is less than 0.1 a.u., showing that the bonds are closed-shell interactions [32]. Moreover, the $-G(r)/V(r)$ ratios are within the range of 0.90 to 0.99, indicating that the H-bonds in all complexes are partially covalent in the gas phase. However, in water as solvent the $-G(r)/V(r)$ ratio is greater than 1 in each complex, except the Ni(II) complexes in which the ratio is less than 1. Therefore, the H-bonds in the Pd(II) and Pt(II) complexes have no appreciable covalent character, whereas those in the Ni(II) complexes are partially covalent.

It can equally be seen from Tables 5 and 6 that for each H-bond in all complexes studied, $\nabla^2\rho(r) > 0$ and $H(r) < 0$, further confirming that all H-bonds listed in these tables are moderate type interactions. The H-bond energies (E_H) have been estimated within the framework of QTAIM, based on the method proposed by Espinosa and co-workers [34]. According to this method, $E_H = ½(V(r))$ where V_{BCP} is the potential energy density at the BCP concerned. The H-bond energies for the investigated complexes calculated via the foregoing method are presented in Tables 5 and 6. The E_H values for each of the complexes studied are higher in the gas phase than in water, and this discrepancy can be attributed to the slight reduction in electron density at the relevant BCPs in water. The E_H values are found to increase in both the gas and the solvent phases in the order: Pt(II) complexes < Pd(II) complexes < Ni(II) complexes, implying that the H-bonds in the Ni(II) complexes are the strongest. The trend of the H-bond energies is similar to that of the chemical hardness values for each series (1-4) of the complexes investigated. It can be therefore concluded that the H-bond strength is one of the key parameters responsible for the stability of the complexes.

The correlations between H-bond length and electron density (ρ), as well as between H-bond length and the Laplacian of electron density ($\nabla^2\rho$) have been determined. These correlations are equally depicted in Fig. 3. Interestingly, good correlation coefficients (R^2) were obtained in each case. In the case of electron density and H-bond length, the R^2 value is 0.990 in the gas phase and 0.991 in water. On the other hand, the R^2 value for H-bond length and $\nabla^2\rho$ is 0.983 and 0.987 in the gas phase and in water, respectively. It is evidenced from the graphs in Fig. 4 that the H-bond lengths are inversely proportional to the electron density, showing that an increase in the interatomic distance results in a reduction in orbital overlap, thus reducing electron density along the bond path. A similar observation was made between the H-bond lengths and the Laplacian of electron density.

In both gas and water phases, the $\rho(\boldsymbol{r})$ values of the M-N coordinative bonds (listed in Tables 5 and 6) range from 0.100-0.124 a.u., indicating that all M-N bonds in the complexes studied are intermediate-type interactions. The values of the ratio $-G(r)/V(r)$ for these M-N bonds are such that $0.5 < -G(r)/V(r) < 1$, showing that these interactions are partially covalent in nature. This conclusion is corroborated by the values of $\rho(\boldsymbol{r})$, which is between 0.1 and 0.2 a.u. The partial covalent nature of these bonds is further confirmed by the fact that $\nabla^2\rho(r) > 0$ and $H(r) < 0$ in both media studied. Furthermore, the M-N interaction energies (listed in Tables 5 and 6), estimated using the approach proposed by Espinosa and co-workers [34], are found to be highest in Pd(II) complexes and lowest in Pt(II) complexes. This shows that the M-N coordinative bonds are stronger in latter complexes than with the rest of the complexes in both media investigated. Since the M-N bonds are strongest in Pt(II) complexes, and the lowest binding energy is also obtained for the formation of this complex, then Pt(II)-binding (in contrast to Pd(II)-binding) by the vic-dioximes ligands investigated is a highly favorable process. Clearly, the M-N interaction energies calculated in water are lower than those obtained in the gas phase for all complexes, suggesting that the presence of water as solvent weakens the M-N bonds owing to solvent-solute interactions.

Infra-Red (IR) Vibrational Analysis

Some gas phase calculated IR frequencies of vic-dioximes ligands and their metal d^8 complexes studied are listed in Table 7. The vibrational band assignments of these frequencies were performed with the aid of the GaussView 5.0.8 molecular visualization program. The experimental FT-IR frequencies of dimethylglyoxime [35] and diphenylglyoxime [36] are also presented in Table 7, for comparison with the theoretical values. To improve the agreement between the calculated IR vibrational frequencies and the experimentally observed wavenumbers, the theoretical values were scaled down using the equation

$$N_{scaled} = 22.1 + 0.9543\ \nu_{calculated} \quad (7)$$

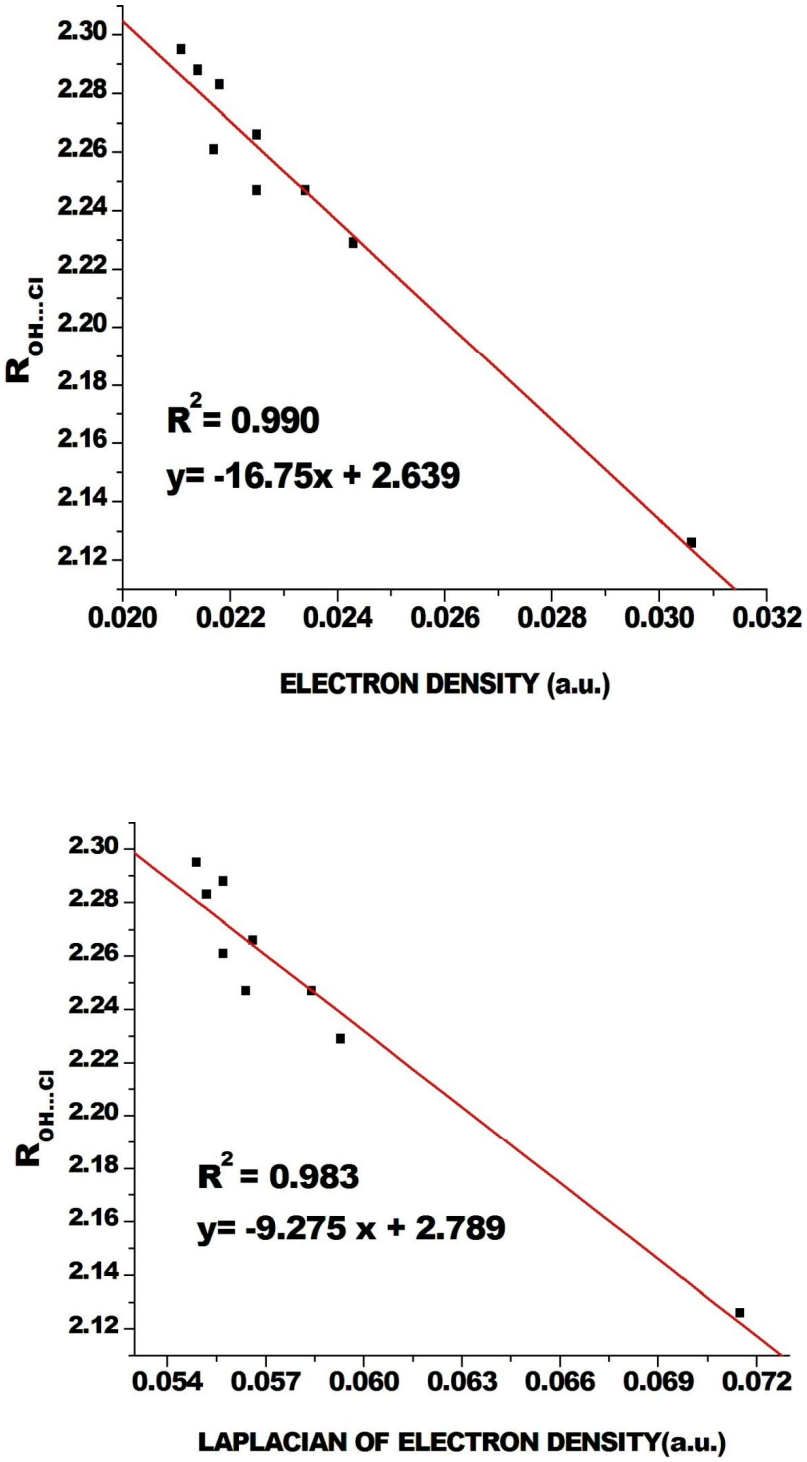

Fig. 4. Linear dependence of H-bond distances at bond critical points in the gas phase with electron density and Laplacian of electron density.

Table 6. Topological Analysis of H-bonds (O-H···Cl) and M-N bonds of the Complexes Studied in Water

Complexes	Interactions	$\rho(r)$	$\nabla^2\rho(r)$	$H(r)$	$-G(r)/V(r)$	E (kJ mol^{-1})
			O-H···Cl/M-N			
Ia	OH···Cl	0.0265	0.0687	-0.00096	0.95	-24.9
	M-N	0.101	0.542	-0.0135	0.92	-212.7
Ib	OH···Cl	0.0181	0.0518	0.00049	1.04	-15.8
	M-N	0.104	0.481	-0.0202	0.87	-211.5
Ic	OH···Cl	0.0179	0.0520	0.000531	1.05	-15.6
	M-N	0.122	0.502	-0.0360	0.82	-258.6
IIa	OH···Cl	0.0313	0.728	-0.00207	0.91	-29.4
	M-N	0.104	0.564	-0.0154	0.91	-225.8
IIb	OH···Cl	0.0188	0.0533	0.000367	1.03	-16.5
	M-N	0.107	0.491	-0.0225	0.86	-220.5
IIc	OH···Cl	0.0184	0.0529	0.000447	1.04	-16.2
	M-N	0.124	0.507	-0.0381	0.81	-266.5
IIIa	OH···Cl	0.0288	0.0726	-0.00143	0.94	-27.4
	M-N	0.104	0.550	-0.0158	0.91	-221.9
IIIb	OH···Cl	0.0202	0.0554	0.000108	1.01	-17.9
	M-N	0.107	0.490	-0.0221	0.87	-219.2
IIIc	OH···Cl	0.0197	0.0549	0.000217	1.02	-17.5
	M-N	0.124	0.510	-0.0383	0.81	-267.8
IVa	OH···Cl	0.0271	0.0699	-0.00108	0.94	-25.7
	M-N	0.104	0.549	-0.0155	0.91	-220.5
IVb	OH···Cl	0.0189	0.0534	0.000345	1.02	-16.7
	M-N	0.107	0.491	-0.0222	0.87	-219.2
IVc	OH···Cl	0.0186	0.0532	0.000422	1.03	-16.4
	M-N	0.125	0.510	-0.390	0.81	-269.1

Table 7. Experimental and Calculated Vibrational Frequencies (cm^{-1}) at the M06/6-31+G(d,p) Level of Theory, and SDD Basis Set for Metal(II)

Molecules	$\bar{\nu}$ (O-H)		$\bar{\nu}$ (C=N)		$\bar{\nu}$ (N-O)		$\bar{\nu}$ (C-C)		$\bar{\nu}$ (C-H)	
	Scaled	Unscaled	Scaled	Unscaled	Scaled	Unscaled	Scaled	Unscaled	Scaled	Unscaled
Ia	3216	3346	1643	1698	1206	1240	1306	1346	3076	3200
Ib	3292	3426	1628	1683	1197	1231	1294	1333	3071	3195
Ic	3311	3446	1609	1662	1169	1202	1295	1334	3087	3212
I	3714	3868	1653	1709	1076	1104	1421	1466	2996	3116
IIa	3221	3352	1662	1719	1196	1230	1331	1372	2991	3111
IIb	3286	3421	1643	1698	1187	1221	1323	1363	2994	3114
IIc	3306	3441	1629	1683	1184	1218	1332	1372	2992	3112
II	3715	3870	1662	1718	1031	1057	1276	1314	2980	3100
II’	3400		1570		1143		-		2931	
IIIa	3211	3341	1641	1696	1148	1180	1347	1388	3074	3198
IIIb	3270	3403	1625	1679	1140	1172	1336	1376	3072	3196
IIIc	3294	3428	1615	1670	1135	1166	1349	1390	3072	3196
III	3712	3867	1647	1702	1012	1037	1300	1339	3063	3187
III’	3306		1620		982		-		-	
IVa	3224	3356	1632	1687	1123	1153	1346	1387	3094	3219
IVb	3295	3429	1621	1675	1118	1148	1330	1371	3094	3219
IVc	3324	3460	1610	1664	1114	1144	1332	1372	3095	3220
IV	3714	3868	1638	1694	1025	1051	1278	1316	3089	3214

The experimental values designated II’ and III’ are the IR vibrational frequencies of the ligands II and III only II’ represents experimental wavenumbers from [35]. III’ represents experimental wavenumbers from [36].

commended by many studies [37-40]. In order to access the extent of the agreement between the calculated IR frequencies (scaled) and the experimentally observed values, the correlation Eq. (7) between these values was determined for the dimethylglyoxime and diphenylglyoxime ligands.

$$\nu_{exp} = 0.869\ \nu_{theor} + 179.49 \quad (8)$$

where ν_{exp} and ν_{theor} represent the calculated (scaled) and experimental vibrational frequencies, respectively.

The strong correlation coefficient ($R^2 = 0.992$) obtained between the theoretical and experimental FT-IR frequencies shows a good linear relationship between these values, thus confirming the suitability of the theoretical method employed in geometry optimization.

It is well-known that the IR vibrational frequency of the

O-H group is very sensitive to the nature of the environment. As such, it shows pronounced shifts in the spectra of hydrogen-bonded species. The optimum absorption region of a non H-bonded (a free hydroxyl group) is 3700-3550 cm^{-1} [41]. When involved in an intra or intermolecular H-bond, the IR stretching band of an O-H group is shifted to the 3550-3000 cm^{-1} region [42]. In the present work, the IR stretching bands of the two O-H groups in the free vic-dioximes ligands appeared in the range 3714-3712 cm^{-1}. After complexation, these O-H stretching bands were found to be shifted toward lower wavelengths in the range 3324-3216 cm^{-1}. This conclusively demonstrates that the O-H groups in all complexes investigated are engaged in intramolecular H-bonding interactions with the neighboring chloride ligands. As can be seen from Table 7, there is a significant shift of the IR band for C=N stretching vibration toward smaller wavenumbers upon complexation of the ligands to all metal ions studied. The complexation of the vic-dioxime ligands to the metal centers via the two azomethine nitrogen atoms is expected to reduce the electron density in the azomethine bond, thus lowering the C=N absorption frequency. Indeed, the C=N peaks of the complexes were found to be shifted toward lower frequencies, suggesting the coordination of the azomethine nitrogen to the metal ions. The N-O vibrational bands in all cases studied occurred in the range 1076-1012 cm^{-1} for the free ligands, but were shifted to higher wavelengths (1206-1114 cm^{-1}) in the complexes. This can be attributed to an increase in electron density in N-O bond.

CONCLUSIONS

A DFT study has been undertaken in the present work with the aim of determining the d^8 metal binding ability of vic-dioxime ligands using Ni(II), Pd(II) and Pt(II) as illustrative examples of d^8 metals. The chelating ability of the vic-dioxime derivatives in the presence of chloride ions as ancillary ligands toward the above-mentioned d^8 metal ions in the gas and aqueous phases was investigated. All complexation reactions were found to be thermo-dynamically favorable and exothermic. Additionally, the reactions were found to be more favorable in the gas phase than in water due to solvent-solute interactions. Interestingly, all complexes investigated adopted square planar geometries stabilized by H-bonds formed between the hydroxyl groups and chloride ligands (OH···Cl).

The metal-ligand and H-bond interactions in the molecules investigated were characterized within the framework of QTAIM. It was found that that these H-bonds are partially covalent in the gas phase but noncovalent in water, except for the nickel complexes in which these interactions are partially covalent in both media. Interestingly, good correlation coefficients were obtained between the H-bond lengths and electron density, as well as between the H-bond lengths and the Laplacian of electron density. NPA analysis revealed the occurrence of ligand-metal charge transfer during the formation of complexes studied. The calculated reactivity descriptors have identified the Ni(II) complexes as the most stable structures among the complexes studied. Negative values obtained for binding energies, Gibbs free energy and enthalpy changes of complexation are indicative of the stability of the complexes, affirming the use of vic-dioximes ligands as potential d^8 transition metal eliminating agents in solution.

ACKNOWLEDGEMENTS

This work was supported by the Research Modernization Grant of the Ministry of Higher Education of Cameroon to which we are very grateful. It also benefited from the financial assistance of the Ministry of External Affairs of India and FICCI (Federation of Indian Chambers of Commerce and Industry) through a CV Raman International Fellowship award (Grant no. 101F102) for African Researchers that was realized at IIT Kanpur, Kanpur, India.

CONFLICT OF INTERESTS

The authors declare that there is no conflict of interests regarding the publication of this paper.

REFERENCES

[1] Lance, K. A.; Goldsby, K. A.; Busch, D. H., Effective new cobalt(II) dioxygen carriers derived from dimethylglyoxime by the replacement of linking protons with difluoroboron (1+). *Inorg. Chem.* **1990**,

29, 4537-4544, DOI: 10.1021/ic00347a041.

[2] Taqui, M. K.; Ramachandraiah, G.; Kumar, S., Mononuclear bis(dimethylglyoximato) ruthenium(III) complexes with different addended axial groups: highly efficient catalysts for water oxidation. *J. Mol. Catal.* **1990**, *45*, 199-205, DOI: 10.1016/0304-5102(90)85039-K.

[3] Taqui, M. K.; Ramachandraiah, G.; Mehta, S., Trans-dioxobis(dimethylglyoximato) ruthenium(VII) perchlorate: an active oxidation catalyst for the electrochemical epoxidation of olefins. *J. Mol. Catal.* **1989**, *50*, 123-129, DOI: 10.1016/0304-5102(89)85056-4.

[4] Thomas, T. W.; Underhill, A. E., Metal-metal interactions in transition metal complexes containing infinite chains of metal atoms. *Chem. Soc. Rev.* **1972**, *1*, 99-105, DOI: 10.1039/CS9720100099.

[5] Caulton, K.G.; Cotton, F.A., Cristal and molecular structure of bis(triphenylphosphine) tetrakis(dimethyl-glyoximato)dirhodium(II) length of a rhodium(II)-to-rhodium(II) single bond. *J. Am. Chem. Soc.* **1971**, *93*, 1914-1918, DOI: 10.1021/ja00737a014.

[6] Gök, Y.; Kantekin, H., Synthesis and characterization of novel (E,E)-dioximes and its mono- and heterotrinuclear complexes. *Acta Chem. Scand.* **1997**, *51*, 664-671, DOI: 10.3891/51-0664.

[7] Gurol, I.; Ahsen, V.; Bekâroğlu, ö., Synthesis of soluble complexes from a tetradentate dithioglyoxime ligand. *J. Chem. Soc.* **1992**, 2283-2286, DOI: 10.1039/DT9920002283.

[8] Schrauzer, G. N.; Kohnle, J., Co-enzyme B12-model, *Chemische Berichte,* **1964**, *97*, 3056-3064, DOI: 10.1002/cber.19640971114.

[9] Kuse, S.; Motomizu, S.; Toei, K., *O*-diketonedioxime compounds as analytical reagents for the spectrophotometric determination of nickel. *Analytica Chimica Acta,* **1974**, *70*, 65-76, DOI: 10.1016/S0003-2670(01)82911-1.

[10] Singh, B. K.; Jetley, U. K.; Sharma, R. K.; Garg, B. S., Synthesis, characterization and biological activity of complexes of 2-hydroxy-3,5-dimethylaceto-phenoneoxime (HDMAOX) with copper(II), cobalt(II), nickel(II) and palladium(II). *Spectrochim. Acta,* **2007**, *68*, 63-73, DOI: 10.1016/j.saa.2006.11.001.

[11] Trendafilova, G. N.; Santiago, L. R.; Sodupe, M., Coordination properties of the oxime analogue of glycine to Cu(II). *J. Phys. Chem.* **2005**, *109*, 5668-5676, DOI: 10.1021/jp050626h.

[12] Yari, A.; Kakanejadifard, A., Spectrophotometric and theoretical studies on complexation of a newly synthesized vic-dioxime derivative with nickel(II) in dimethylformamide. *J. Coord. Chem.* **2007**, *60*, 1121-1132, DOI: 10.1080/00958970 601110469.

[13] Zülfikaroğlu, A.; Yüksektepe, C. A.; Hümeyra, B.; Büyükgüngör, O., Experimental and computational studies of bis[bis(2-furyl)glyoximato]nickel(II). *J. Coord. Chem.* **2012**, *65*, 1525-1538, DOI: 10.1080/00958972.2012.675432

[14] Chakravorty, A., Structural chemistry of transition metal complexes of oximes. *Coord. Chem. Rev.* **1974**, *13*, 1-46, DOI: 10.1016/S0010-8545(00)80250-7.

[15] Shridhar, V.; Satyanarayana, S., Coenzyme B_{12} model studies: an HSAB approach to the equilibria and kinetics of axial ligation of alkyl(aquo)-cobaloximes by imidazole and cyanide. *Proc. Ind. Acad. Sc.* **2000**, *112*, 579-591.

[16] Nogheu, L. N.; Ghogomu, J. N.; Mama, D. B.; Nkungli, N. K.; Younang, E.; Gadre, S., Structural, spectral (IR and UV-Vis) and thermodynamic properties of some 3d transition metal(II) chloride complexes of glyoxime and its derivatives: A DFT and TD-DFT study. *Comput. Chem.* **2016**, *4*, 119-136, DOI: 10.4236/cc.2016.44011.

[17] Cirtina, D., Study of the synthesis of some alkyl-aromatic dioximes and their analytical applications. *J. Univ. Chem. Tech. and Met.* **2011**, *46*, 419-422.

[18] Kabanda, M. M.; Van, T. T.; Kamogelo, M. S.; Kemoabetswe, R. N. S.; Tshepiso, J. T.; Quoc, T. T.; Eno, E. E., Conformational, electronic and antioxidant properties of lucidone, linderone and methyllinderone: DFT, QTAIM and NBO studies. *Mol. Phy.* **2015**, *113*, 683-697, DOI:10.1080/00268976.2014.969343.

[19] Bader, R. F. W., Atoms in molecules: a quantum theory, Oxford University Press, Oxford, England: 1990.

[20] Billes, F.; Holmgren, A.; Mikosch, H., A combined DFT and vibrational spectroscopy study of the nickel

and zinc O,O-diethyldithiophosphate complexes. *Vib. Spect.* **2010**, *53*, 296-306, DOI: 10.1016/ j.vibspec.2010.04.011.

[21] Frisch, M. J.; Trucks, G. W.; Schlegel, H. B.; Scuseria, G. E.; Robb, M. A.; Cheeseman, J. R.; Scalmani, G.; Barone, V.; Mennucci, B.; Petersson, G. A.; Nakatsuji, H.; Caricato, M.; Li, X.; Hratchian, H. P.; Izmaylov, A. F.; Bloino, J.; Zheng, G.; Sonnenberg, J. L.; Hada, M.; Ehara, M.; Toyota, K.; Fukuda, R.; Hasegawa, J.; Ishida, M.; Nakajima, T.; Honda, Y.; Kitao, O.; Nakai, H.; Vreven, T.; Montgomery Jr., J. A.; Peralta, J. E.; Ogliaro, F.; Bearpark, M.; Heyd, J. J.; Brothers, E.; Kudin, K. N.; Staroverov, V. N.; Kobayashi, R.; Normand, J.; Raghavachari, K.; Rendell, A.; Burant, J. C.; Iyengar, S. S.; Tomasi, J.; Cossi, M.; Rega, N.; Millam, J. M.; Klene, M.; Knox, J. E.; Cross, J. B.; Bakken, V.; Adamo, C.; Jaramillo, J.; Gomperts, R.; Stratmann, R. E.; Yazyev, O.; Austin, A. J.; Cammi, R.; Pomelli, C.; Ochterski, J. W.; Martin, R. L.; Morokuma, K.; Zakrzewski, V. G.; Voth, G. A.; Salvador, P.; Dannenberg, J. J.; Dapprich, S.; Daniels, A. D.; Farkas, O.; Foresman, J. B.; Ortiz, J. V.; Cioslowski, J.; Fox, D.J., Gaussian 09, Revision A.02. Gaussian, Inc., Wallingford, 2009.

[22] Roy, D. D.; Todd, A. K.; John, M. M., Gauss View 5.0.8, Gaussian, Inc., Wallingford, 2009.

[23] Yan, Z.; Truhlar, D. G., The m06 suite of density functionals for main group thermochemistry, thermochemical kinetics, noncovalent interactions, excited states, and transition elements: two new functionals and systematic testing of four m06-class functionals and 12 other functional. *Theo. Chem. Account.* **2007**, *120*, 215-241, DOI: 10.1007/s00214-007-0310-x.

[24] Hay, P. J.; Wadt, W. R., *Ab initio* effective core potentials for molecular calculations, potentials for the transition metals atoms Sc to Hg. *J. Chem. Phy.* **1985**, *82*, 270-283, DOI: 10.1063/1.448799.

[25] Cancès, E.; Mennucci, B.; Tomasi, J., A new integral equation formalism for the polarizable continuum codel: theoretical background and applications to isotropic and anisotropic dielectrics. *J. Chem. Phy.* **1997**, *107*, 3032-3041, DOI: 10.1063/1.474659.

[26] Tian, L.; Feiwu, C., Multiwfn: A Multifunctional Wavefunction Analyzer. *J. Comp. Chem.* **2012**, *33*, 580-592, DOI: 10.1002/jcc.22885.

[27] Ayres, P. W.; Parr, R. G., Vibrational principles for describing chemical reactions: the fukui function and chemical hardness. *J. Am. Chem. Soc.* **2000**, *122*, 2010-2018, DOI: 10.1021/ja9924039.

[28] Bader, R. F. W.; Anderson, S. G.; Duke, A. J., Quantum topology of molecular charge distributions. *J. Am. Chem. Soc.* **1979**, *101*, 1389-1395, DOI: 10.1021/ja00500a006.

[29] Bader, R. F. W.; Slee, T. S.; Cremer, D.; Kraka, E., Description of conjugation and hyperconjugation in terms of electron distributions. *J. Am. Chem. Soc.* **1983**, *105*, 5061-5068, DOI: 10.1021/ja0035IIIa035.

[30] Bader, R. F. W.; MacDougall, P. J.; Lau, C. D. H., Bonded and nonbonded charge concentrations and their relation to molecular geometry and reactivity. *J. Am. Chem. Soc.* **1984**, *106*, 1594-1605, DOI: 10.1021/ ja00318a009.

[31] Bader, R. F. W.; MacDougall, P. J., Toward a theory of chemical reactivity based on charge density. *J. Am. Chem. Soc.* **1985**, *107*, 6788-6795, DOI: 10.1021/ ja00310a007.

[32] Farrugi, L. J.; Kocovsky, P.; Senn, H. M.; Vyskocil, S., Weak intra- and intermolecular interactions in a binaphthol imine: an experimental charge-density study on (±)-8'-benzhydrylideneamino-1,1'-binaphthyl-2-ol. Acta Crystallographica sect. B. **2009**, *65*, 757-769, DOI: 10.1107/S010876810903273x.757.

[33] Koch, U.; Popelier, P. L. A., Characterization of C-H-O hydrogen bonds on the basis of the charge density. *J. Phy. Chem.* **1995**, *99*, 9747-9754, DOI: 10.1021/j10002IVa016.

[34] Espinosa, E.; Molins, E.; Lecomte, C., Hydrogen bond strengths revealed by topological analyses of experimentally observed electron densities. *Chem. Phy. Lett.* **1998**, *285*, 170-173, DOI: 10.1016/S0009-2614(98)0036-0.

[35] Shayma, A.; Shaker, Preparation and spectral properties of mixed-ligand complexes of VO(IV), Ni(II), Zn(II), Pd(II), Cd(II) and Pb(II) with dimethylglyoxime and N-acetylglycine. *E-J. Chem.* **2010**, *7*, 580-586.

[36] Naomi, P.; Ndahi, A.; Kolawole, A., Cobalt(III) complexes of diphenylglyoxime as possible non-organometallic models of vitamin B12. *J. Sc.* **2005**, *101*, 457-463.

[37] Palafox, M. A.; Rastogi, V. K., Quantum chemical predictions of the vibrational spectra of polyatomic molecules, the uracil molecule and two derivatives. *Spectrochim. Acta A.* **2002**, *58*, 411-440, DOI: 10.1016/S1386-1425(01)00509-1.

[38] Palafox, M. A., Scaling factors for the prediction of vibrational spectra of Benzene molecule. *Int. J. Quant. Chem.* **2000**, *77*, 661-684, DOI: 10.1002/(SICI)1097-461x.

[39] Palafox, M. A.; Nunez, J. L.; Gil, M., Accurate scaling of the vibrational spectra of aniline and several derivatives. *J. Mol. Struct.* **2002**, *593*, 101-131, DOI: 10.1016/S0166-1280(02)00319-6.

[40] Ambrish, K.; Anoop, K. P.; Narayana, B. K.; Sarojini, S. P.; Nayak, M., Normal modes, molecular orbitals and thermochemical analyses of 2,4- and 3,4-dichloro substituted phenyl-N-(1,3-thiazol-2-yl) acetamides: DFT study and FTIR spectra. *J. Theo. Chem.* **2014**, *2014*, 1-10, DOI: 10.1155/2014/125841.

[41] Panicker, C. Y.; Varghese, H. T.; Ambujakshan, K. R.; Mathew, S.; Ganguli, S.; Nanda, A. K.; Van Alsenoy, C., FT-IR and FT-Raman spectra and *ab initio* calculations of 3-{[(2-hydroxyphenyl) methylene]amino}-2-phenylquinazolin-4(3H)-one. *J. Raman Spect.* **2009**, *40*, 1262-1273, DOI: 10.1002/jrs.2276.

[42] Teimouri, A. N.; Chermahini, A.; Taban, K.; Dabbagh, H., Experimental and CIS, TD-DFT, *ab initio* calculations of visible spectra and the vibrational frequencies of sulfonylazide-azoic dye''. *Spectrochim. Acta Part A.* **2009**, *72*, 369-377, DOI: 10.1016/j.saa.2008.10.006.